

Research Article

BQ-Chem: A Quantum Software Program for Chemistry Simulation Based on the Full Quantum Eigensolver Algorithm

Hang Li ,¹ Pan Gao,¹ Jiang Zhang,¹ Zhiyuan Liu,¹ Hai Wei,² Kai Wen ,² Shijie Wei ,¹ and Gui-Lu Long ,^{1,3,4,5}

¹Beijing Academy of Quantum Information Sciences, Beijing 100193, China

²Beijing QBoson Quantum Technology Co., Ltd., Beijing 100015, China

³State Key Laboratory of Low-Dimensional Quantum Physics and Department of Physics, Tsinghua University, Beijing 100084, China

⁴Beijing National Research Center for Information Science and Technology and School of Information Tsinghua University, Beijing 100084, China

⁵Frontier Science Center for Quantum Information, Beijing 100084, China

Correspondence should be addressed to Kai Wen; wenk@boseq.com, Shijie Wei; weisj@baqis.ac.cn, and Gui-Lu Long; gllong@mail.tsinghua.edu.cn

Received 20 July 2022; Revised 21 October 2022; Accepted 28 October 2022; Published 7 December 2022

Academic Editor: Guo-Xing Miao

Copyright © 2022 Hang Li et al. This is an open access article distributed under the Creative Commons Attribution License, which permits unrestricted use, distribution, and reproduction in any medium, provided the original work is properly cited.

We describe a quantum chemistry simulation software program *BQ-Chem*, which can calculate the low-energy spectrum and potential energy surface of molecules on a quantum computer. *BQ-Chem* is based on the full quantum eigensolver (FQE), which is implemented with a quantum gradient descent algorithm. Benefiting from FQE, *BQ-Chem* can perform all the calculations on a quantum computer. Compared with the classical optimization methods which encounter the optimization difficulty of high-dimensional and multivariable functions in dealing with multielectron orbitals of macromolecules, FQE provides an exponential speedup. FQE works fully on a quantum computer; thus, *BQ-Chem* can be smoothly transited to future large-scale quantum computers.

1. Introduction

Quantum chemistry is also called molecular quantum mechanics, where quantum mechanics is applied to the field of chemistry to obtain the chemical properties of molecules at the atomic level. A central challenge in the field of quantum chemistry is to determine the low-lying molecular energies and electronic structures of a chemical system with high precision, and its electronic Hamiltonian usually can be obtained with a set of nuclear geometries under the Born–Oppenheimer approximation. Moreover, by varying nuclear positions of a chemical system, a potential energy surface (e.g., ground-state energy) can be determined as a function of the bond length or bond angle of interest, which is key to understanding chemical reactivity, product distributions, and reaction rates.

Conventionally, the number of classical bits needed to simulate a multatom molecule increases exponentially as the number of atoms. And in the worst case, quantum simulation of a chemical system is exponentially hard on classical computers. Despite the great success of approximation methods, tackling the problem accurately with conventional computers is still a difficult task. On the other hand, the chemistry of molecules is accurately described with quantum mechanics; thus, the quantum simulation of a chemical system with a quantum simulator or quantum computer has natural advantages in the sense of computational resources needed [1, 2].

However, the problem of estimating the ground state and its energy of Hamiltonian is in general QMA-hard [3] and even quantum computers are not expected to efficiently solve it. In the past few decades, various quantum algorithms

are harnessed to address this issue. The main idea of these methods is to prepare a state which extremely approximates to the desired ground state instead of preparing the exact ground state which is computationally expensive. Based on the well-known adiabatic theorem [4, 5] and quantum phase estimation algorithm [6], Aspuru-Guzik et al. [7, 8] constructed an adequate quantum circuit to evolve the system adiabatically in the ground state, i.e., adiabatic state preparation. The quantum imaginary time evolution algorithm [9, 10], which uses the linear combination of unitaries (LCU) [11] formalism, is another approach as a heuristic method to approximate the ground state.

Despite developments in quantum algorithms and optimization of resource requirements, many of the algorithms have hardware requirements far beyond the capability of near-term quantum computers. In 2014, a quantum-classical hybrid algorithm called variational quantum eigensolver (VQE) [12, 13] was proposed by Peruzzo et al. VQE can prepare a class of ansatz states with a variational quantum circuit and optimize its parameters, leading the state approximating to the ground state step by step. VQE requires fewer quantum gates and a shallower circuit, making it more feasible on noisy intermediate-scale quantum (NISQ) [14] devices. In 2020, Wei et al. developed a full quantum eigensolver (FQE) [15] scheme which attracted much attention in recent years [16–21]. Compared with VQE where its optimization step is completed on a classical computer, FQE, using the quantum gradient descent algorithm in the LCU paradigm, is a fully quantum algorithm where the calculation of the expectation value of Hamiltonian and the optimization process is fully conducted on quantum computers, enabling it an advantage of providing a smooth transition to future large-scale quantum computers.

2. BQ-Chem

Here, we give an introduction to a newly designed quantum chemistry simulation software program *BQ-Chem* (<https://biwonq.baqis.ac.cn/#/pages/chemistry>), which is based on FQE. This quantum chemistry simulation module supports multitask parallel computing, and users can edit their specific contents after adding projects on the main page.

2.1. Specifying a Molecule and Its Parameters. In order to simplify the process and improve the user's experience of the program, we preinstalled the specific molecular configures of about 50 common molecules for users as default in *BQ-Chem*, including the atomic type, the x , y , and z coordinate of each atomic nucleus, and the bonding properties between them. The default data of chemical compositions and their parameters about our preinstalled molecules are extracted from the National Institute of Standards and Technology (NIST) Chemistry WebBook (<https://webbook.nist.gov/chemistry/>) of the United States. In addition, users are also allowed to build their own molecular models flexibly by adding more atoms and changing atomic coordinates and corresponding bonding properties, as shown in Figure 1, where we take NH_3 molecule as an example of specifying a molecule and its parameters in *BQ-Chem*.

2.2. Two Calculation Modes. After specifying a molecule and its parameters from the last step, users can calculate the chemical properties of the molecule of their interest. The *BQ-Chem* simulation module supports two calculation modes for users to choose from: the static single-point energy spectrum (SES) calculation mode where all molecular geometry parameters given are fixed and the dynamic potential energy surface (PES) calculation mode where some molecular parameters of the user's interest range around the given geometry. As the following shows, the SES mode supports calculating the ground and excited energies sequentially, while the PES mode supports calculating the ground energy around the given geometry by varying the bond length or bond angle of a molecule. In both modes, one should first set the preprocessing information, including basis set choice, fermion-spin transformation model choice, and the initial state choice.

2.2.1. Single-Point Energy Spectrum (SES) Mode. In the mode of SES, one can choose to calculate the ground-state energy with FQE and up to 15 excited-level energies one by one by subtracting the ground-state energy part from the system Hamiltonian and calculating the new ground-state energy of the subtracted Hamiltonian.

BQ-Chem provides several classical methods for preprocessing molecular electronic structures for users. As depicted in Figure 2, the following steps are taken:

- (1) Choosing the single-electron atomic orbital basis set from the option of “sto-3g” and “sto-6g.” Here, we take “sto-*ng*” atomic orbitals instead of the original “sto” or “gto” basis, which means the basis functions are expressed as sums of Gaussian functions rather than the original Slater-type orbitals to enhance the efficiency of integral evaluation. More details are described in Appendix A.
- (2) Choosing the Fermi-spin transformation method from Jordan–Wigner or Bravyi–Kitaev transformation. The Jordan–Wigner transformation directly maps the fermionic occupation state of a particular atomic orbital to a state of qubits, while the Bravyi–Kitaev transformation is a compromise between the Jordan–Wigner transformation and the parity encoding transformation, which is more efficient in operational complexity. More details are described in Appendix C.
- (3) Choosing the initial state of the full quantum eigensolver solution process from the option of the Hartree–Fock approximation state or the uniform superposition state. The Hartree–Fock approximation state usually is a better choice for faster convergence. More details are described in Appendix B.

We take NH_3 molecule as an example; its configuration and setting of the SES mode are shown in Figure 2, i.e., Hartree–Fock state as the initial state, “sto-6g” as the basis, Jordan–Wigner transformation method as the chosen Fermi-spin transformation, and the goal is to obtain the ground energy and up to three excitation energies.

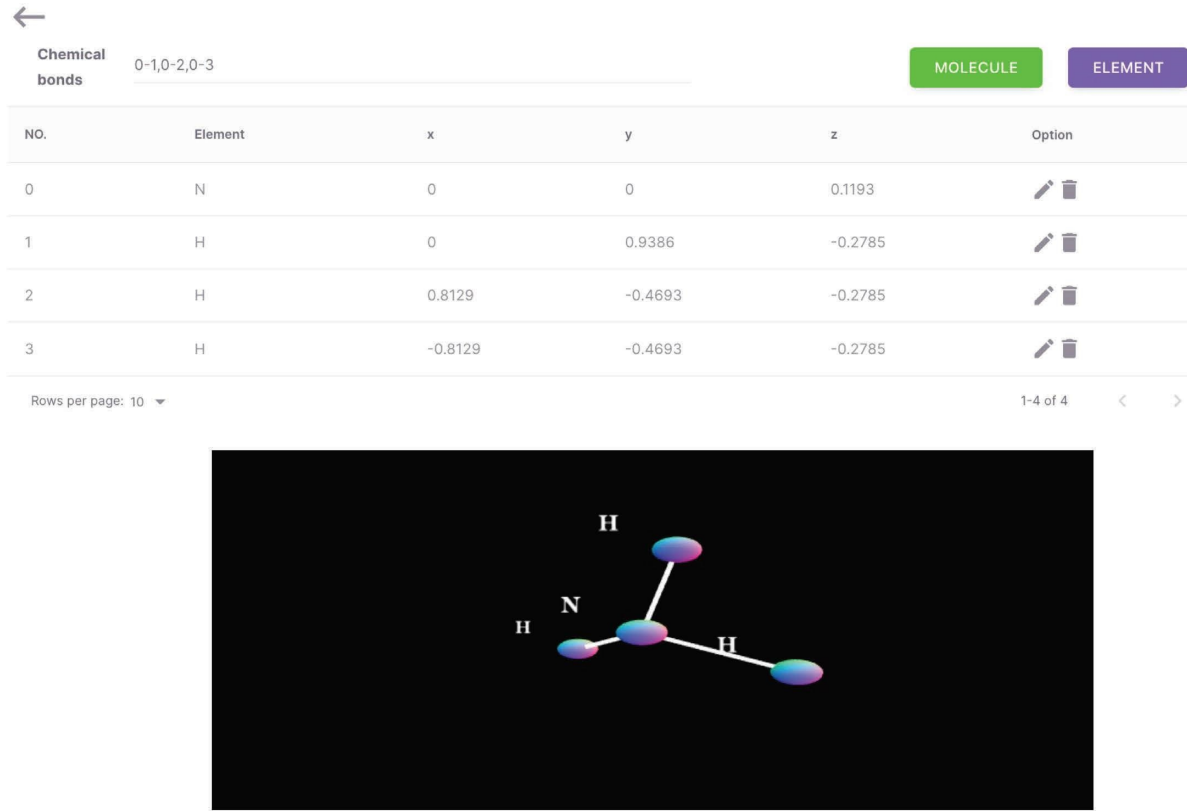


FIGURE 1: Input interface of the NH_3 molecular data as an example in the *BQ-Chem* simulation module. One can select a molecule structure from a preset database and modify the structure by changing the coordinates of its element. One can also construct another molecule structure by adding or deleting an atom from the selected molecular structure.

After executing the process, a resultant spectrum of 4 energy levels is presented in Figure 3, where we can see as the iteration of the quantum gradient descent algorithm increases, the simulated ground-state and up to three excitation energies have a convergence to the theoretical energies of the interested Hamiltonian, respectively. To be noted, the ground-state energy can be obtained directly from the original Hamiltonian with FQE, while the 1st excitation energy is acquired from a new Hamiltonian by reducing the ground-state energy part of the original Hamiltonian with the same FQE process. By repeating the above process, one can reach any excited-level energy one after the other.

2.2.2. Potential Energy Surface (PES) Mode. In the mode of PES, one can choose the scanning mode from “bond length” and “bond angle”; moreover, one can set the scanning number and scanning field, as depicted in Figure 4. If the “bond length” option is selected, one is further required to provide which set of chemical bonds is going to be modified. Otherwise, if the “bond angle” option is selected, one is further required to specify two chemical bonds which share a common atom (as the vertex of two connected edges).

We take NH_3 molecule as an example again. Its configuration and setting of the PES mode are shown in Figure 4, i.e., “bond length” as the scanning option, all chemical

bonds of NH_3 are specified, and 11 scanning points of chemical bond length set ranging from 50% to 150% of the original chemical bond length and its setting are maintained the same with the SES mode.

PES can help search for the most stable structure of the interested molecule by ranging the length and angles of the chemical bonds, which is very useful in the field of biomedicine, materials, and chemical industry. In the example of calculating PES of the NH_3 molecule, the resultant PES as presented in Figure 5 shows that the molecule with the original set of chemical bond lengths has the lowest energy which is the most stable structure of NH_3 molecule under the fixed chemical bond angles.

3. Full Quantum Eigensolver

In this section, we will give a detailed description of the underlying algorithm in the *BQ-Chem* module, FQE. A diagram of FQE for solving the ground-state energy of a molecule is depicted in Figure 6. As discussed above, the word “full” for FQE [15] means that all computations of FQE are realized on quantum computers, while other eigensolvers require a sequence of data transformation between quantum computers and classical computers. The reason why FQE can be fully completed on a quantum computer is that it takes advantage of the technology of linear combination of unitary operators (LCU) which is proposed by Long in 2002 [11].

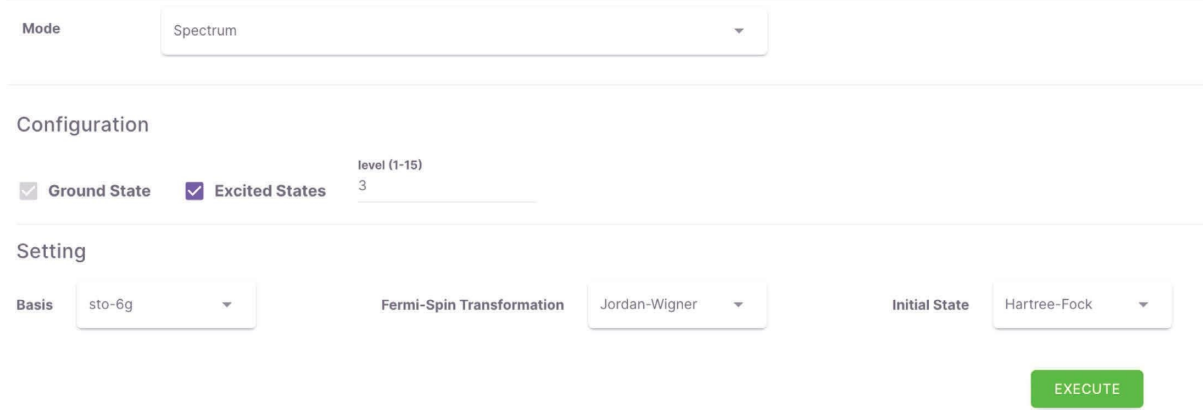


FIGURE 2: Input interface of the SES mode in the *BQ-Chem* simulation module. One can modify the configuration and setting to specify the spectrum calculation mode.

LCU can realize the four arithmetic operations, addition, subtraction, multiplication, and division of unitary operators.

After the secondary quantization, the fermion Hamiltonian of the molecule is transformed into the qubit Hamiltonian in the Hilbert space through mathematical mapping. The ground state of the Hamiltonian can be obtained by applying the FQE. In a specific quantum computing system, we shall choose a suitable initial quantum state, then construct a quantum circuit realizing the quantum gradient descent process, and measure the final quantum state to obtain the information that the next loop is required. In the process of continuous iteration of the quantum circuit, the final state converges to the ground state of our interested Hamiltonian. On the other hand, searching for the most stable structure of a molecule is very difficult in quantum chemistry and requires massive classical computation. Similar to solving the ground state energy problem, FQE can also be used to find the state with the lowest energy by changing the distance between atoms or angles between chemical bonds in a molecule and obtain the most stable structure of the molecule.

A molecular system containing nuclei and electrons can be described by its molecular Hamiltonian. Through Jordan-Wigner (JW) or Bravyi-Kitaev (BK) transformation, the molecular Hamiltonian can be mapped to the Hamiltonian in a qubit form.

$$H = \sum_{i,\alpha} \omega_{\alpha}^i \sigma_{\alpha}^i + \sum_{i,j,\alpha,\beta} \omega_{\alpha\beta}^{ij} \sigma_{\alpha}^i \sigma_{\beta}^j + \dots, \quad (1)$$

where the Roman indices i, j denote the qubit on which the operators act and Greek indices α, β refer to the type of Pauli operators; for example, σ_x^i means Pauli matrix σ_x acting on the i -th qubit. Apparently, H in equation (1) is a linear combination of unitary Pauli matrices. We can calculate the ground-state energy by minimizing the expected value of the Hamiltonian.

$$f(\vec{X}) = \vec{X}^T H \vec{X}. \quad (2)$$

The following methods for finding the molecular ground state and its energy are all based on it.

In classical computing, we usually use the gradient descent algorithm to obtain the minimum value of the objective function $f(\vec{X})$. We start from the initial state $\vec{X}^{(0)} \in \mathbb{R}^N$ and evolve along the object function's gradient direction to the next state:

$$\vec{X}^{(t+1)} = \vec{X}^{(t)} - \gamma_0 \nabla f(\vec{X}^{(t)}). \quad (3)$$

In the case of solving the ground-state energy of the Hamiltonian problem with FQE, the gradient of $f(\vec{X})$ can be expressed as follows:

$$\nabla f(\vec{X}) = 2H\vec{X}. \quad (4)$$

And, the iterative process of classical gradient descent can be mapped into a quantum version, which can be considered as the evolution of the quantum state \vec{X} under the operator H .

$$\left| \vec{X}^{(t+1)} \right\rangle = \left(\left| \vec{X}^{(t)} \right\rangle - \gamma H \left| \vec{X}^{(t)} \right\rangle \right), \quad (5)$$

where $\gamma = 2\gamma_0$.

We define a new Hamiltonian as follows:

$$H^g = I - \gamma H = \sum_{i=1}^M \beta_i H_i^g, \quad (6)$$

where M is the number of Pauli terms of operator H^g . The process of the quantum gradient descent algorithm can be expressed as follows:

$$\left| \vec{X}^{(t+1)} \right\rangle = H^g \left| \vec{X}^{(t)} \right\rangle = \sum_{i=1}^M \beta_i H_i^g \left| \vec{X}^{(t)} \right\rangle. \quad (7)$$

H^g is an LCU operator, which is a nonunitary evolution and can be realized on a quantum computer by adding auxiliary qubits to convert it into a unitary evolution in a larger Hilbert space. The entire quantum circuit diagram described by equation (7) is divided into four parts as shown in Figure 7:

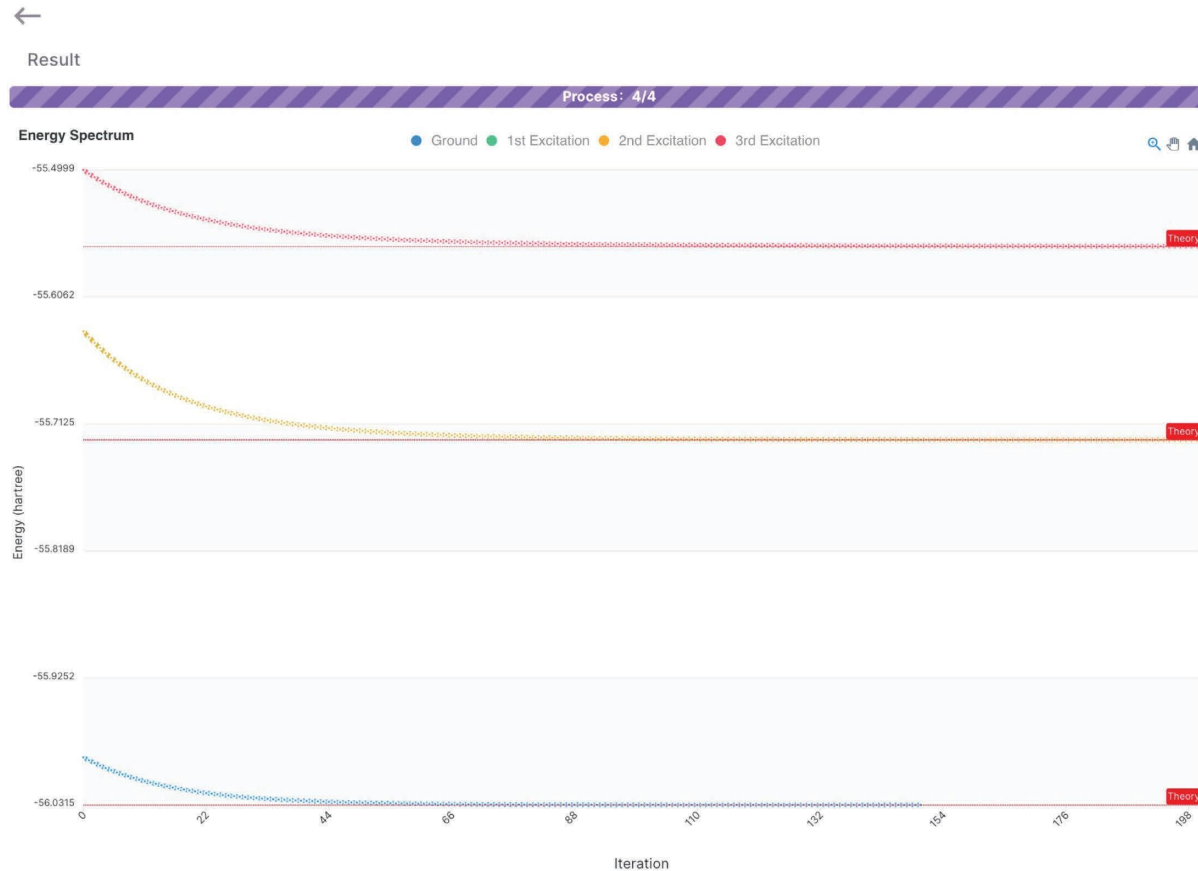


FIGURE 3: The resulting energy spectrum of the ground state (blue dotted line) and up to the 3rd excitation state (green, yellow, and red dotted line) of NH_3 in BQ-Chem. Each dotted line converges monotonically to the theoretical value of the exact Hamiltonian diagonalization energy (red-solid line), respectively. To be noted, the 1st excitation energy curve (green) is covered by the 2nd excitation energy curve (yellow) of molecule NH_3 due to their degeneracy; thus, the green line cannot be seen directly.

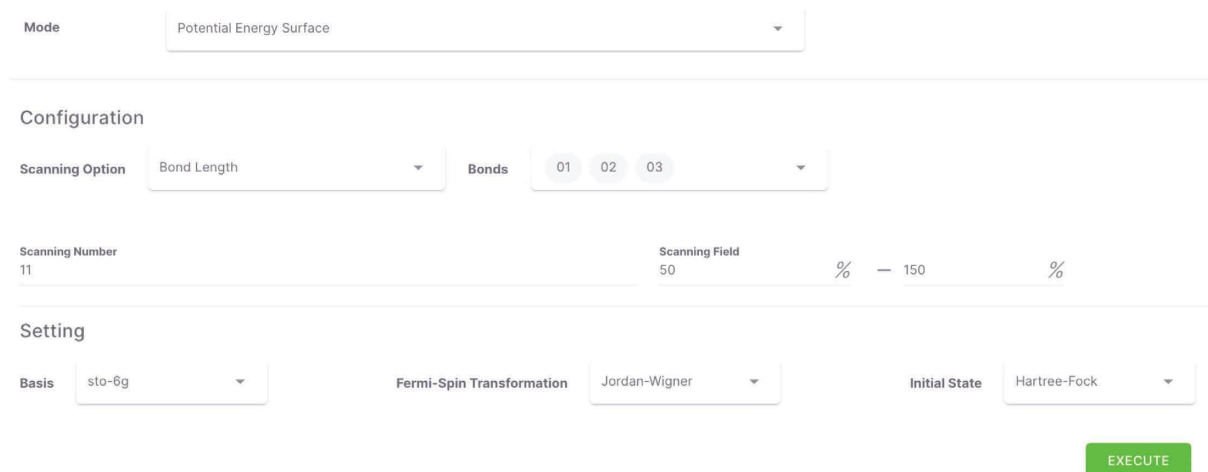


FIGURE 4: Input interface of potential energy surface calculation in the BQ-Chem simulation module. One can modify the configuration and setting to specify the potential energy surface calculation mode.

Wave division: The entire quantum system is composed of a work system and an ancillary system. Firstly, we encode the initial vector $X = (x_1, \dots, x_N)^T$ into the initial state $|x^{(t)}\rangle$ of the work system. In the field of

quantum chemistry, the Hartree-Fock (HF) state is often adopted as an initial state. The ancillary system is initialized from $|0^m\rangle$, where $m = \log_2 M$, to a specific superposition as follows:

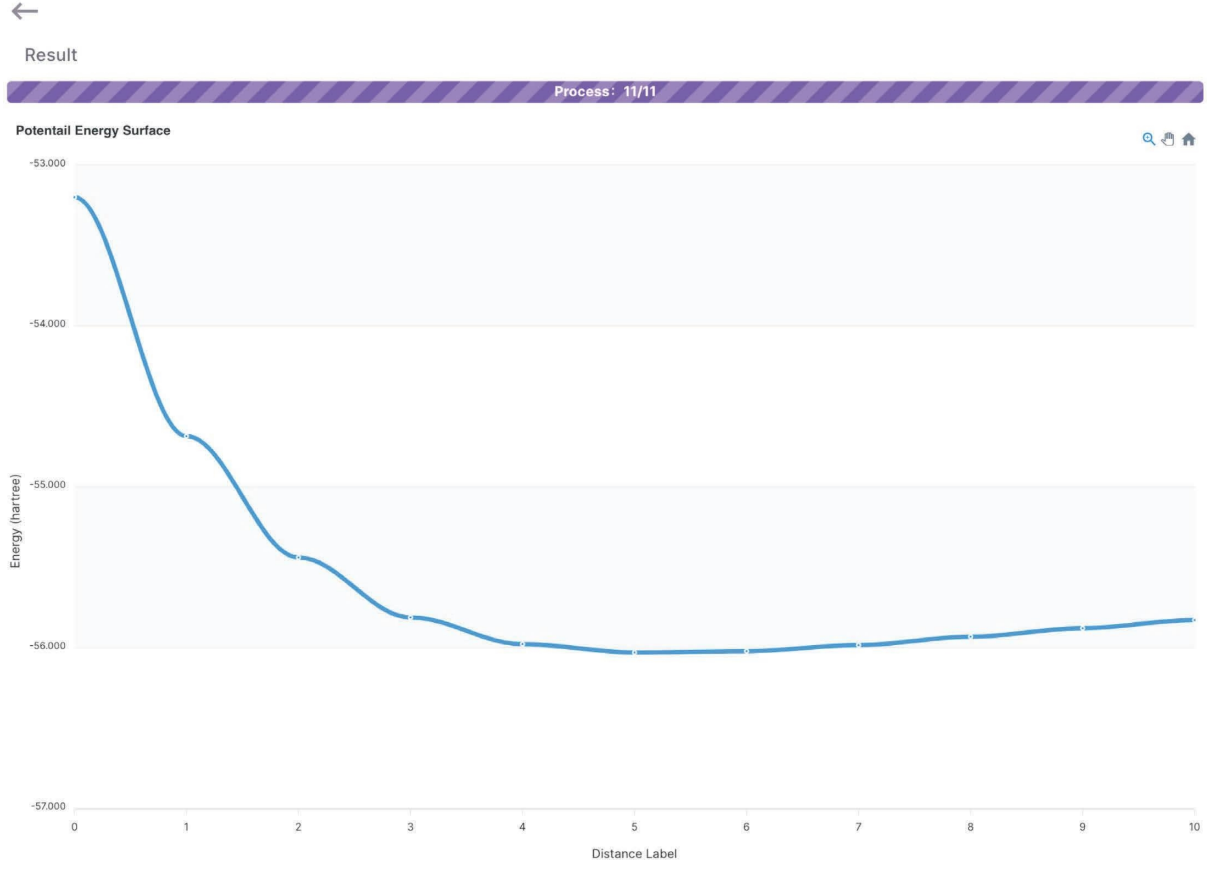


FIGURE 5: The resultant potential energy surface of NH_3 based on FQE corresponding to different chemical bond length sets ranging from 50% to 150% of the original chemical bond length. The energy corresponding to the 5-th scanning point (the exact original chemical bond length set) has the lowest value, suggesting the most stable structure of NH_3 molecule.

$$|\psi_s\rangle = \frac{1}{C} \sum_{i=0}^{M-1} \beta_i |i\rangle. \quad (8)$$

Here, $C = \sqrt{\sum_{i=0}^{M-1} \beta_i^2}$ is a normalization constant and $|i\rangle$ is the computational basis. We denote the composite state of the whole system as $|\Phi\rangle = |\psi_s\rangle |\vec{x}^{(t)}\rangle$.

Entanglement: A series of ancilla-controlled operations $\sum_{i=0}^{M-1} |i\rangle\langle i| \otimes H_i^g$ on the work qubits are implemented, the work qubits and the ancillary qubits are now entangled, and the state is transformed into

$$|\Phi\rangle \longrightarrow \frac{1}{C} \left(\sum_{i=0}^{M-1} \beta_i |i\rangle H_i^g |\vec{x}^{(t)}\rangle \right). \quad (9)$$

Wave combination: After performing m Hadamard gates on the ancillary register, the state of the whole system in the subspace where the ancillary system in state $|0\rangle$ is

$$|\Phi_0\rangle = \frac{1}{C\sqrt{2^m}} \left(|0\rangle \sum_{i=0}^{M-1} \beta_i H_i^g |\vec{x}^{(t)}\rangle \right). \quad (10)$$

Measurement: Here, we make measurements on the ancillary register. If $|0\rangle$ is detected, our algorithm

succeeds and we obtain the state $(1/(\mathbb{C}\sqrt{2^m}))(|0\rangle \sum_{i=0}^{M-1} \beta_i H_i^g |\vec{x}^{(t)}\rangle) \propto |\vec{x}^{(t+1)}\rangle$, which is proportional to the next iterative state. The probability of success in detecting the ancillary state in $|0\rangle$ is

$$P_s = \frac{\|H^g |\vec{x}^{(t)}\rangle\|^2}{C^2 M}. \quad (11)$$

After successfully obtaining $|0\rangle$ in the ancillary system, we can continue the gradient descent process by repeating the above four steps. We can preset a threshold of $\varepsilon = |\langle \vec{x}_t | H | \vec{x}_t \rangle - \langle \vec{x}_{t+1} | H | \vec{x}_{t+1} \rangle| / |\langle \vec{x}_t | H | \vec{x}_t \rangle|$ as the criterion for stopping the iteration. After enough iterations, the final state of work system $|X\rangle$ will converge to our interested Hamiltonian H 's ground state and $\langle X | H | X \rangle$ is the corresponding ground state energy.

The successful probability after n -time measurements is $1 - ((\mathbb{C}^2 M - \|H^g |\vec{x}^{(t)}\rangle\|^2) / \mathbb{C}^2 M)^n$, which is an exponential function of n . The number of measurements is $\mathbb{C}^2 M / \|H^g |\vec{x}^{(t)}\rangle\|^2$, which shows its complexity will grow exponentially with respect to the number of iteration steps [22], which is a relatively large limitation and should be solved in future work.

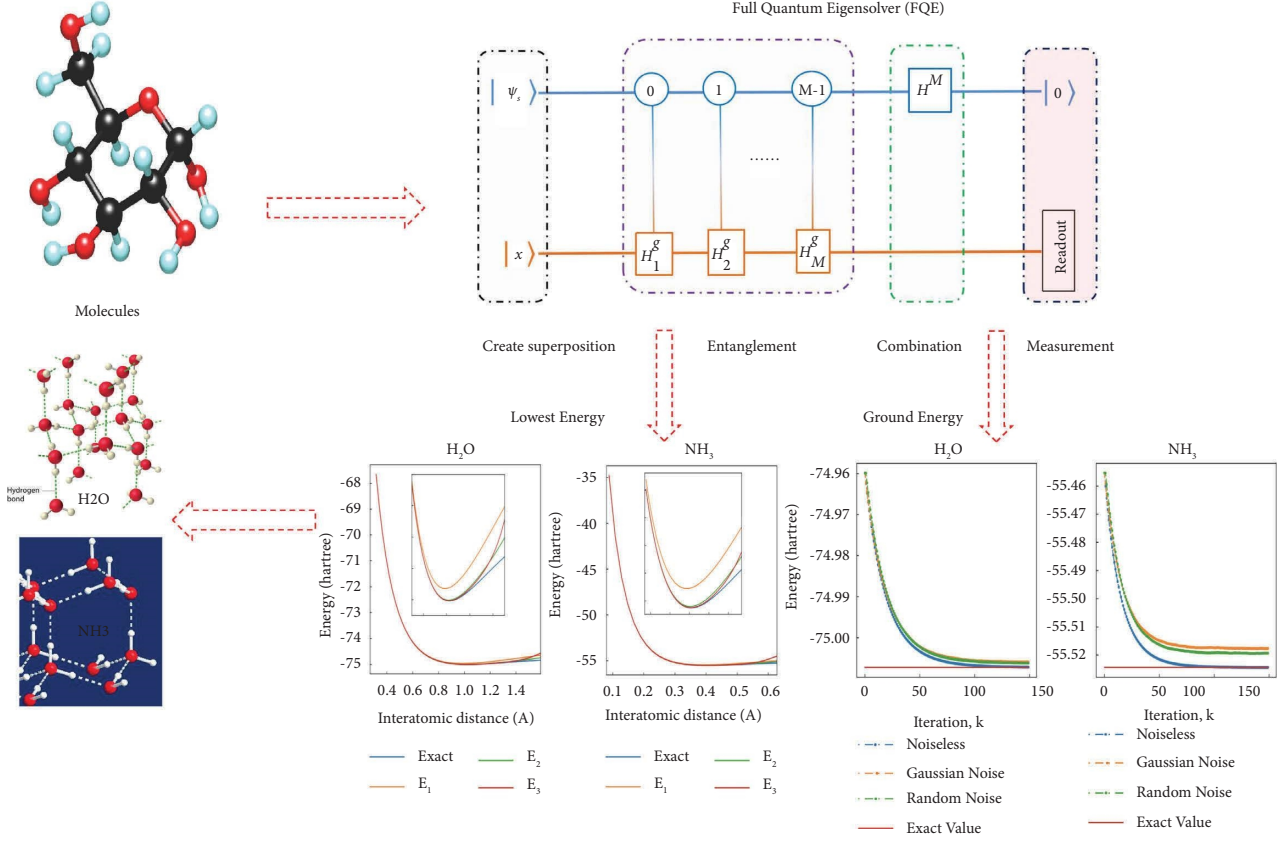


FIGURE 6: Schematic diagram for the process of solving the ground state energy of a molecule. The molecular Hamiltonian is obtained through quantum chemistry software, such as OpenFermion. And then, the ground state energy of the Hamiltonian is calculated through the FQE. By changing the interatomic distances or angles between chemical bonds of a molecule, the method can calculate the most stable structure of the molecule and its corresponding potential energy surface.

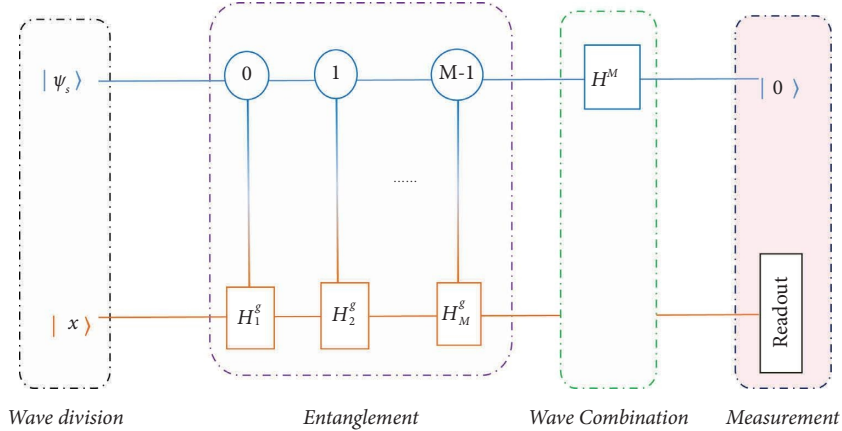


FIGURE 7: Quantum circuit for realizing the quantum gradient descent algorithm. $|\psi_s\rangle$ and $|x\rangle$ ($|\vec{x}^t\rangle$) are the initial states of the ancillary system and the work system, respectively, the controlled operations of the ancillary system acting on the work system are $\sum_{i=0}^{M-1} |i\rangle\langle i| \otimes H_i^g$, and H^M denotes $m = \log_2 M$ Hadamard gates. At the end of the circuit, the final state of the ancillary register is measured. If all ancillary qubits are measured in $|0\rangle$, then the work system collapses in $|\vec{x}^{(t+1)}\rangle$.

4. Summary

In this paper, we present a quantum chemical simulation software program based on FQE and *BQ-Chem*. With *BQ-Chem*, we can calculate the single-point energy spectrum

(SES) and potential energy surface (PES) after specifying the configuration and setting of a molecule. In the SES mode, we can obtain the ground-state energy directly with FQE. In addition, we can calculate the excited states and energies by replacing the interested Hamiltonian with the original

Hamiltonian after reducing the part corresponding to its ground state following the same procedure. In PES mode, by varying the distances between atoms or angles between the chemical bonds in a molecule, we can search for the lowest energy and the corresponding most stable structure of a molecule with a set of distances or angles, from its potential energy surface corresponding to different distances or angles.

Appendix

A. Basis Set

In quantum chemical calculations based on the self-consistent field method (SCF), the single-electron orbital basis vectors of molecules are generally approximated by the linear combination of the single-electron orbital basis vectors (basis set) of each constituent atom. We know that for a hydrogen-like atom with nuclear electron number Z , its single-electron wave function takes the form

$$\psi_{nlm} = R_{nl}(r)Y_{lm}(\theta, \varphi), \quad (\text{A.1})$$

where the radial function

$$R_{nl}(r) = \sqrt{\left(\frac{2Z}{na_\mu}\right)^3 \frac{(n-l-1)!}{2n((n+l)!^3)} e^{-Zr/na_\mu}} \left(\frac{2Z}{na_\mu}\right)^l L_{n-l-1}^{2l+1}\left(\frac{2Zr}{na_\mu}\right), \quad (\text{A.2})$$

and $a_\mu = 4\pi\epsilon_0\hbar^2/\mu e^2$ [23]. Since the mass of the nucleus can be regarded as infinite relative to the mass of the electron, the reduced mass can be approximately taken as the mass of the electron, i.e., $\mu = m_n m_e / (m_n + m_e) \approx m_e$; then, a_μ is the corresponding Bohr radius. A generalized Laguerre function can be expressed as follows:

$$L_{n-l-1}^{2l+1}(x) = (-1)^{2l+1} \frac{d^{2l+1}}{dx^{2l+1}} \frac{e^x}{(n+l)!} \frac{d^{n+l}}{dx^{n+l}}(x^{n+l} e^{-x}). \quad (\text{A.3})$$

Besides, the angular function in equation (A.1) is

$$Y_{lm}(\theta, \varphi) = (i)^{m+|l|} \sqrt{\frac{2l+1}{4\pi} \frac{(l-|l|)!}{(l+|l|)!}} P_{lm}(\cos \theta) e^{im\varphi}, \quad (\text{A.4})$$

where $i = \sqrt{-1}$ is the imaginary symbol, and the adjoint Legendre polynomial has the form

$$P_{lm}(x) = (1-x^2)^{|l|/2} \frac{d^{|l|}}{dx^{|l|}} \frac{1}{2^l l!} \frac{d^l}{dx^l}(x^2 - 1)^l. \quad (\text{A.5})$$

A.1. Slater-Type Orbitals (sto). Generally speaking, the single-electron radial wave function of a hydrogen-like atom of equation (A.2) is extremely complex and difficult to handle in numerical calculations. For this reason, John C. Slater simplified the radial function part of equation (A.1) approximately [24, 25] as follows:

$$R_n(r, \zeta) = N r^{n-1} e^{-\zeta r}, \quad (\text{A.6})$$

which becomes the basis set of Slater-type orbitals function (sto). We have the following:

- (i) $N = (2\zeta)^n \sqrt{2\zeta/(2n)!}$ is the normalization coefficient
- (ii) n is the principal quantum number
- (iii) r is the radial distance between the electron and the atomic kernel
- (iv) ζ is a constant related to the effective nuclear charge determined by Slater's rule

After substituting equations (A.4) and (A.6) into equation (A.1), the "sto" basis set is obtained. As we can see, "sto" has a natural physical meaning; thus, the approximation is better.

A.2. Gaussian-Type Orbitals (gto). The Gaussian-type orbitals (gto) set is another typical atomic electron orbital basis set. Boys [26, 27] first reduced the radial wave function in (A.2) to

$$R_n(r, \alpha) = N r^{n-1} e^{-\alpha r^2}, \quad (\text{A.7})$$

where N , n , and r take the same definition as equation (A.6) and α is a constant number related to the effective nuclear charge.

According to the Gaussian Product Theorem, the product of any two Gaussian functions (gtos) centered at two different positions can be replaced by a finite sum of gtos centered on a point along the axis connecting them. When we select the "gto" basis set, the molecular electronic state of the n -atom molecule can be expressed as the product of n "gto" atomic electronic states at n nuclei centers, respectively. According to the *Gaussian Reproduction Lemma*, the product can be further expressed as the linear superposition of Gaussian integral function production with $n/2$ centers and again further expressed as the linear superposition of multiple Gaussian integral function productions with the same center. In other words, the computational efficiency of the "gto" basis set is much higher than that of the sto basis set, and this advantage can sometimes reach 4–5 orders of magnitude. However, by comparing equation (A.6) with (A.7), as shown in Figure 8, it can be found that the two function properties near $r = 0$ are quite different, which means that although the computational efficiency of "gto" is higher than that of "sto," its computational accuracy is lower than that of "sto."

A.3. "sto- ng " Atomic Orbitals. In order to solve the problem that the Gaussian function does not match the linearity of real atomic orbitals, a "gto" orbit can be approximated by the linear superposition of multiple Gaussian orbits with different parameters α [28, 29]. These "sto" orbitals participating in the superposition are called the primitive Gaussian basis set, and their linear superposition is called the contracted Gaussian basis set, where the superposition coefficients are obtained and fixed by prior optimization. It remains unchanged in the subsequent variational

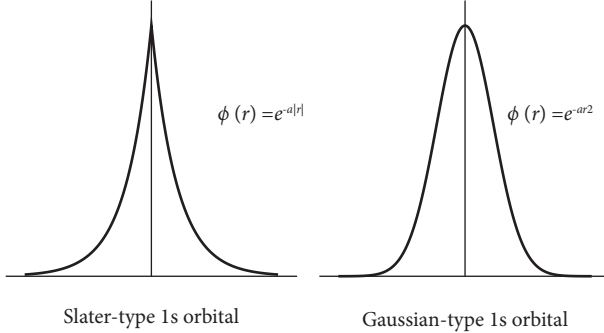


FIGURE 8: Linear comparison of radial functions of “sto” and “gto.”

optimization process for finding the ground state of the molecule; i.e., the superposition coefficient is not used as an optimization parameter.

Generally, the approximate “sto” atomic orbital basis set obtained by the linear superposition of n Gaussian basis vectors is denoted by “sto- ng .” For example, as depicted in Figure 9, “sto-3g” is a linear superposition of three Gaussian-type atomic orbitals to approximate a Slater-type atomic orbital.

$$\psi_{sto-3g} = \left(c_1 e^{-\alpha_1 r^2} + c_2 e^{-\alpha_2 r^2} + c_3 e^{-\alpha_3 r^2} \right) r^{n-1} Y_{l,m}. \quad (A.8)$$

B. Hartree–Fock Self-Consistent Field Method

In Appendix A, we get the basis set $\{\phi_k^i(r)\}$, where $\phi_k^i(r)$ represents the i -th single-electron atomic orbital of the k -th atom. A single-electron molecular orbital $\phi^j(r) = \sum_k c_{k,i}^j \phi_k^i(r)$ can be obtained by linearly superposing different one-electron atomic orbitals. After the direct product of different single-electron molecular orbitals and the commutative antisymmetry operation, a multielectron molecular orbital that satisfies fermion statistics can be obtained.

$$\Psi(r_1, r_2, \dots, r_n) = \frac{1}{\sqrt{n!}} \sum_{\sigma=1}^{n!} (-1)^\sigma P_\sigma [\phi^{j_1}(r_1) \phi^{j_2}(r_2) \cdots \phi^{j_n}(r_n)], \quad (B.1)$$

where P_σ is the commutation operation, and equation (B.1) is the Slater determinant.

Under the Born–Oppenheimer approximation, we regard the nucleus as stationary and only provide a background electrostatic field for the electrons; then, the multielectron Hamiltonian of the molecule can be expressed as follows:

$$H = H_0 + H_I = \sum_i \left(-\frac{1}{2} \nabla_i^2 - \sum_a \frac{Z_a}{r_{i,a}} \right) + \sum_{i < j} \frac{1}{r_{i,j}}. \quad (B.2)$$

H_0 is the potential energy of the kinetic energy of the electron under the background electric field, that is, the single energy, and H_I describes the Coulomb potential energy between the electrons. The energy of the corresponding many-body quantum state Ψ is expressed as follows:

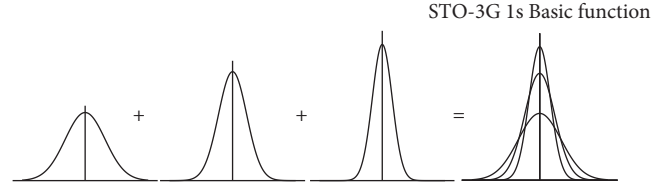


FIGURE 9: An example radial function diagram of sto-3g, which is composed of 3 superimposed original Gaussian functions.

$$E_\Psi = \langle \Psi | H_0 | \Psi \rangle + \langle \Psi | H_I | \Psi \rangle = E_0 + E_I. \quad (B.3)$$

For the zero-order approximation E_0 , since the direct product state $|\varphi^1|\varphi^2 \cdots |\varphi^n\rangle$ is an eigenstate of H_0 , E_0 can be directly described as the summation of single-particle energies.

$$E_0 = \sum_{i=1}^n \langle \phi^i | -\frac{1}{2} \nabla_i^2 - \sum_a \frac{Z_a}{r_{i,a}} | \phi^i \rangle. \quad (B.4)$$

H_I is the interaction Hamiltonian, expressed as

$$\begin{aligned} E_I &= \frac{1}{2 \cdot N!} \sum_{i \neq j}^n \sum_{\sigma} (-1)^{\sigma+\omega} \langle \phi^{P_\sigma(i)} | \langle \phi^{P_\sigma(j)} | \frac{1}{r_{i,j}} | \phi^{P_\omega(i)} \rangle | \phi^{P_\omega(j)} \rangle, \\ &= \frac{1}{2} \sum_{i \neq j}^n \langle \phi^i | \langle \phi^j | \frac{1}{r_{i,j}} | \phi^i \rangle | \phi^j \rangle - \frac{1}{2} \sum_{i \neq j}^n \langle \phi^i | \langle \phi^j | \frac{1}{r_{i,j}} | \phi^j \rangle | \phi^i \rangle. \end{aligned} \quad (B.5)$$

In principle, the corresponding many-body ground state and ground state energy can be obtained by calculating the minimum of equation (B.3) with calculus of variations. We know that the many-body state $|\Psi\rangle$ is obtained by the Slater symmetrization of the single-electron molecular state $|\varphi^i\rangle$, and then, the variation of equation (B.3) is actually the variation of $|\varphi^i\rangle$. Considering the normalization condition of the one-electron molecular state, equations (B.5) and (B.5) can be substituted into equation (B.3), and the Lagrangian multiplier term can be matched at the same time:

$$- \sum_{i,j=1}^n \varepsilon^{i,j} (\langle \phi^i | \phi^j \rangle - \delta_{i,j}). \quad (B.6)$$

After a variation of the whole system on a certain state $\langle \varphi^i |$ and taking the extreme $\delta E / \delta \langle \varphi^i | = 0$, there should be

$$\begin{aligned} &\left\{ \left[-\frac{1}{2} \nabla_t^2 - \sum_a \frac{Z_a}{r_{t,a}} \right] + \left[\sum_{j \neq i}^n I \otimes \langle \phi^j | \frac{1}{r_{i,j}} I \otimes | \phi^j \rangle \right], \right. \\ &\left. \left[\sum_{j \neq i}^n I \otimes \langle \phi^j | \frac{1}{r_{i,j}} | \phi^j \rangle \otimes I \right] \right\} | \phi^i \rangle = \sum_{j=1}^n \varepsilon^{i,j} | \phi^j \rangle, \end{aligned} \quad (B.7)$$

which is the Hartree–Fock self-consistent field equation [30, 31]. For the Hermitian matrix $\varepsilon^{i,j}$, there always exists a unitary transformation U that can diagonalize it, and then, if we take $\sum_{j=1}^n U_{i,j} | \phi^j \rangle$ as the new φ^i , a regular form Hartree–Fock equation can be expressed as

$$F_i|\varphi^i\rangle = (h_i + J_i - K_i)|\varphi^i\rangle = \varepsilon^i|\varphi^i\rangle, \quad (\text{B.8})$$

where F_i is the i -th row of the Fock operator F that has a dependency on the single-electron state $\{|\varphi^i\rangle\}$, ε^i is the i -th eigenvalue of F , and

$$h_i = -\frac{1}{2}\nabla_i^2 - \sum_a \frac{Z_a}{r_{i,a}}, \quad (\text{B.9})$$

is the monomer energy of the i -th single-electron state,

$$J_i = \sum_{j \neq i}^n I \otimes \langle \phi^j | \frac{1}{r_{i,j}} I \otimes | \phi^j \rangle, \quad (\text{B.10})$$

is the Coulomb repulsion energy of the i -th single-electron state corresponding to other electrons, and

$$K_i = \sum_{j \neq i}^n I \otimes \langle \phi^j | \frac{1}{r_{i,j}} | \phi^j \rangle \otimes I, \quad (\text{B.11})$$

is the Fermi exchange energy between the i -th single-electron state and other electronic states.

The variational optimization process of the Hartree–Fock method can be depicted as the flowchart in Figure 10:

- (1) Start from the preset single-electron molecular state $\{|\varphi^i\rangle\}$
- (2) Calculate the corresponding Fock operator $F(\{|\varphi^i\rangle\})$ according to equations (B.9)–(B.11)
- (3) Diagonalize the Fock operator F to get the corresponding eigenvectors $\{|\varphi'\rangle\}$ and eigenvalues
- (4) Continue to substitute the new single-electron molecular state as in (2) to obtain a new F' until convergence

C. Fermi-Spin Transformation Method

Quantum simulation of chemistry is always dealing with fermions that satisfy the Pauli exclusion principle (i.e., electrons) [32, 33]. We can simply handle the electrons of spin $\uparrow\downarrow$ as handling two different kinds of spin-free fermions without spin-orbit coupling. In this section, spin-free fermions are used as an example to introduce related calculation methods. Since fermions satisfy commutative antisymmetry,

$$\begin{aligned} & \{f_i^\dagger, f_j\} \\ & \{f_i, f_j\} = \{f_i^\dagger, f_j^\dagger\} = 0. \end{aligned} \quad (\text{C.1})$$

However, as the basic storage unit of a quantum computer, the qubit is a boson that satisfies commutative symmetry, i.e., SU (2) spin, which satisfies

$$\begin{aligned} & [\sigma_i^+, \sigma_j^-] \\ & [\sigma_i^+, \sigma_j^+] = [\sigma_i^-, \sigma_j^-] = 0. \end{aligned} \quad (\text{C.2})$$

By comparing equation (C.1) with equation (C.2) and combining the occupation properties of the fermion state

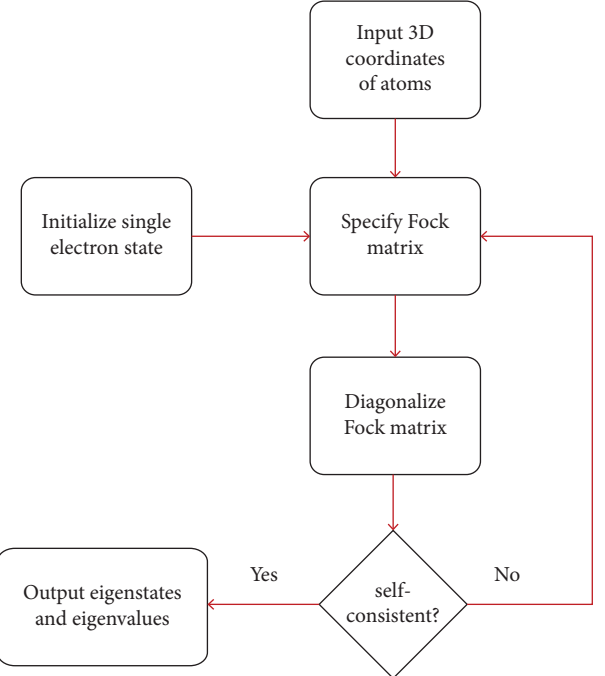


FIGURE 10: Schematic diagram of the process of Hartree–Fock self-consistent solution.

and the state directivity of the 1/2 spin, we can form an equation between the single-fermion operators f_i and f_i^\dagger and the 1/2–SU (2) spin operators σ_i^+ , σ_i^- , and σ_i^z as follows:

$$\begin{cases} f_i^\dagger \longrightarrow \sigma_i^+, \\ f_i \longrightarrow \sigma_i^-, \\ f_i^\dagger f_i \longrightarrow \frac{1}{2}(1 + \sigma_i^z). \end{cases} \quad (\text{C.3})$$

This shows that if only the particles on the same lattice are considered, the Fock state basis vector $|0, 1\rangle$ of the Fermi system and the spin basis vector $|\downarrow, \uparrow\rangle$ can be one-to-one correspondence, and furthermore, its Hamiltonian can be related to each other with the same transformation.

However, the situation could be quite different when dealing with multiple-lattice Fermi systems, the structure obtained from equation (C.3) loses the commutative anti-symmetry property of fermions, which will cause confusion of sign in the calculation, leading to completely wrong results. In that sense, a unitary operation that faithfully connects the fermionic Fock space with the spin space is required. Obviously, such a unitary transformation cannot be local.

C.1. Jordan–Wigner Transformation. Considering the fermions as a one-dimensional chain, we can denote the fermion lattice as $i = 0, 1, \dots, n - 1$ based on the algebras of fermion particles. In order to unify the sign of Fermi-spin

operators on the j -th lattice, we can just calculate the parity of all fermions occupied before the j -th lattice and then assign it to the local operators of the j -th lattice, which is exactly the Jordan–Wigner transformation and its inverse is shown in equation (C.4). We can simply verify that the Jordan–Wigner transformation [34–36] is a global unitary transformation.

$$\begin{cases} \left(\prod_{i < j} \sigma_j^z \right) \sigma_j^+ \longrightarrow f_j^\dagger, \\ \left(\prod_{i < j} \sigma_j^z \right) \sigma_j^- \longrightarrow f_j, \\ \frac{1 + \sigma_j^z}{2} \longrightarrow f_j^\dagger f_j. \end{cases} \quad (\text{C.4})$$

Because of the existence of string operators ($\prod_{i < j} (1 - 2f_i^\dagger f_i)$) and ($\prod_{i < j} \sigma_j^z$) in equation (C.4), the averaged number of spin operators required to encode a fermion operator is linear to the system size under the Jordan–Wigner transformation; i.e., the Jordan–Wigner transformation has an encoding complexity of $O(n)$.

C.2. Bravyi–Kitaev Transformation. When encoding the fermionic operators with spin operators, two pieces of information should be included, the fermionic occupation on i -th lattice and the fermionic parity of i -th lattice (i.e., the parity of the fermionic occupation numbers of all lattices preceding i -th lattice). The Jordan–Wigner transformation encodes the fermionic occupation information with the local spin operator σ_j^z and encodes the fermionic occupation number parity information with the nonlocal string operator $\prod_{i < j} \sigma_j^z$. Another protocol called “Parity encoding” is in the opposite encoding way, where the local spin operator at j -th lattice encodes into the parity of the fermionic occupation numbers at all lattices up to and including lattice number j and encodes the spin string operator into the occupation state at the j -th fermionic lattice. Similar to the Jordan–Wigner transformation, the parity encoding of the Bravyi–Kitaev transformation [37–39] also has a linear averaged complexity of $O(n)$.

In order to reduce the encoding complexity of fermion operators in the spin formula, Bravyi and Kitaev [40] proposed another Fermi–spin transformation method in 2002, namely, the Bravyi–Kitaev transformation, which is a compromise between the Jordan–Wigner transformation and the parity encoding transformation. The Bravyi–Kitaev method draws on the binary tree structure to encode the information of the Fermi subsystem on the spin system, as shown in Figure 11, where the solid gray lines represent the left branches, the dashed black lines represent the right branches, and the solid red circles are

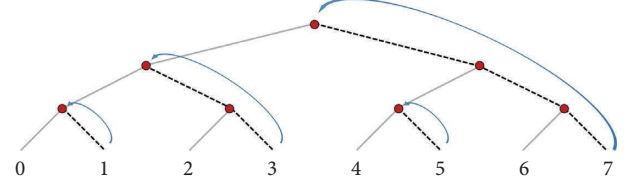


FIGURE 11: Diagram of encoding rules for the Bravyi–Kitaev transformation.

the roots. At the bottom layer of Figure 11, the spin state at the j -th (i.e., even j) lattice on the left branch stores the local occupation information of the fermion chain at the same j -th lattice and the right branch at the j -th (i.e., odd j) lattice stores the fermion occupation number parity information for some finite sets of the lattices, which conclude all lattices under the root of the highest level that can be reached along the right branch route starting from the j -th lattice.

Under the Bravyi–Kitaev transformation, the Fock state basis vector $|f_0, f_1, \dots, f_{2^n-1} (f_i = 0, 1)$ can be connected with the spin state $|s_0, s_1, \dots, s_{2^n-1} (s_i = \uparrow, \downarrow)$ by a transformation matrix β_{2^n} .

$$\beta_{2^n} = \begin{pmatrix} \beta_{2^{n-1}} & 0 \\ K & \beta_{2^{n-1}} \end{pmatrix}, K = \begin{pmatrix} 0 \\ 1, 1, \dots, 1 \end{pmatrix}, \beta_1 = (1). \quad (\text{C.5})$$

We take 8 lattices as an example in Figure 11; the Bravyi–Kitaev transformation can be expressed as follows:

$$\begin{pmatrix} s_0 \\ s_1 \\ s_2 \\ s_3 \\ s_4 \\ s_5 \\ s_6 \\ s_7 \end{pmatrix} = \begin{pmatrix} 1 & 0 & 0 & 0 & 0 & 0 & 0 & 0 \\ 1 & 1 & 0 & 0 & 0 & 0 & 0 & 0 \\ 0 & 0 & 1 & 0 & 0 & 0 & 0 & 0 \\ 1 & 1 & 1 & 1 & 0 & 0 & 0 & 0 \\ 0 & 0 & 0 & 0 & 1 & 0 & 0 & 0 \\ 0 & 0 & 0 & 0 & 1 & 1 & 0 & 0 \\ 0 & 0 & 0 & 0 & 0 & 0 & 1 & 0 \\ 1 & 1 & 1 & 1 & 1 & 1 & 1 & 1 \end{pmatrix} \begin{pmatrix} f_0 \\ f_1 \\ f_2 \\ f_3 \\ f_4 \\ f_5 \\ f_6 \\ f_7 \end{pmatrix} = \begin{pmatrix} f_0 \\ f_0 \oplus f_1 \\ f_2 \\ f_0 \oplus \dots \oplus f_3 \\ f_4 \\ f_4 \oplus f_5 \\ f_6 \\ f_0 \oplus \dots \oplus f_7 \end{pmatrix}, \quad (\text{C.6})$$

where \oplus is a symbol of modulo-2 binary addition. Obviously, $\beta_{2^n} \beta_{2^n}^\dagger \neq \mathbb{I}$ means that β_{2^n} is not a unitary transformation; nevertheless, it is always linearly invertible.

By applying the conjugate of the transformation matrix β to the fermionic Hamiltonian, the spin Hamiltonian with the same energy spectrum can be obtained and thus solved on a quantum computer. Under the Bravyi–Kitaev transformation, the fermionic single lattice occupation number information and the parity information are stored neither locally in the single lattice of spins nor in the string operator with linear complexity, but in the string operator with logarithmic length. This means the averaged encoding complexity of the fermionic creation and annihilation operators under the Bravyi–Kitaev transformation is $O(\log n)$.

Data Availability

The data sets generated and/or analyzed during the current study are available from the corresponding author on reasonable request.

Conflicts of Interest

The authors declare that they have no conflicts of interest.

Acknowledgments

This work was supported by the National Natural Science Foundation of China (Grant nos. 12005015 and 12004206).

References

- [1] P. Benioff, “The computer as a physical system: a microscopic quantum mechanical Hamiltonian model of computers as represented by turing machines,” *Journal of Statistical Physics*, vol. 22, no. 5, pp. 563–591, 1980.
- [2] R. P. Feynman, “Simulating physics with computers,” *International Journal of Theoretical Physics*, vol. 21, no. 6-7, pp. 467–488, 1982.
- [3] A. Yu Kitaev, A. Shen, M. N. Vyalyi, and M. N. Vyalyi, *Classical and Quantum Computation*, American Mathematical Society, USA, 2002.
- [4] D. M. Tong, K. Singh, L. C. Kwek, and C. H. Oh, “Quantitative conditions do not guarantee the validity of the adiabatic approximation,” *Physical Review Letters*, vol. 95, no. 11, Article ID 110407, 2005.
- [5] D. M. Tong, K. Singh, L. C. Kwek, and C. H. Oh, “Sufficiency criterion for the validity of the adiabatic approximation,” *Physical Review Letters*, vol. 98, no. 15, Article ID 150402, 2007.
- [6] M. A. Nielsen and I. L. Chuang, *Quantum Computation and Quantum Information*, Cambridge University Press, Cambridge, U, 2010.
- [7] A. Aspuru-Guzik, A. D. Dutoi, P. J. Love, and M. Head-Gordon, “Simulated quantum computation of molecular energies,” *Science*, vol. 309, no. 5741, pp. 1704–1707, 2005.
- [8] R. Babbush, P. J. Love, and A. Aspuru-Guzik, “Adiabatic quantum simulation of quantum chemistry,” *Scientific Reports*, vol. 4, no. 1, pp. 6603–6611, 2014.
- [9] M. Motta, C. Sun, A. T. K. Tan et al., “Determining eigenstates and thermal states on a quantum computer using quantum imaginary time evolution,” *Nature Physics*, vol. 16, no. 2, pp. 205–210, 2020.
- [10] S. McArdle, T. Jones, S. Endo, Y. Li, S. C. Benjamin, and X. Yuan, “Variational ansatz-based quantum simulation of imaginary time evolution,” *npj Quantum Information*, vol. 5, no. 1, pp. 75–76, 2019.
- [11] L. Gui-Lu, “General quantum interference principle and duality computer,” *Communications in Theoretical Physics*, vol. 45, no. 5, pp. 825–844, 2006.
- [12] A. Peruzzo, J. McClean, P. Shadbolt et al., “A variational eigenvalue solver on a photonic quantum processor,” *Nature Communications*, vol. 5, no. 1, pp. 4213–4217, 2014.
- [13] J. R. McClean, J. Romero, R. Babbush, and A. Aspuru-Guzik, “The theory of variational hybrid quantum-classical algorithms,” *New Journal of Physics*, vol. 18, no. 2, Article ID 023023, 2016.
- [14] J. Preskill, “Quantum computing in the nisq era and beyond,” *Quantum*, vol. 2, p. 79, 2018.
- [15] S. Wei, H. Li, and G. L. Long, “A full quantum eigensolver for quantum chemistry simulations,” *Research: Ideas for Today's Investors*, vol. 2020, pp. 1–11, 2020.
- [16] A. Tranter, P. J. Love, F. Mintert, N. Wiebe, and P. V. Coveney, “Ordering of trotterization: impact on errors in quantum simulation of electronic structure,” *Entropy*, vol. 21, no. 12, p. 1218, 2019.
- [17] D. Chivilikhin, A. Samarin, V. Ulyantsev, I. Iorsh, A. R. Oganov, and O. Kyriienko, “Mog-vqe: multiobjective genetic variational quantum eigensolver,” 2007.04424, 2020.
- [18] A. Robert, P. Kl. Barkoutsos, S. Woerner, and I. Tavernelli, “Resource-efficient quantum algorithm for protein folding,” *npj Quantum Information*, vol. 7, no. 1, pp. 38–45, 2021.
- [19] S. E. Smart and D. A. Mazziotti, “Quantum solver of contracted eigenvalue equations for scalable molecular simulations on quantum computing devices,” *Physical Review Letters*, vol. 126, no. 7, Article ID 070504, 2021.
- [20] S. Jin, S. Wu, G. Zhou et al., “A query-based quantum eigensolver,” *Quantum Engineering*, vol. 2, no. 3, p. e49, 2020.
- [21] Z. Hu, X. Liu, M. Tian et al., “Recent progress and new perspectives for diterpenoid biosynthesis in medicinal plants,” *Medicinal Research Reviews*, vol. 41, no. 6, pp. 2971–2997, 2021.
- [22] P. Rebentrost, M. Schuld, L. Wossnig, F. Petruccione, and S. Lloyd, “Quantum gradient descent and Newton's method for constrained polynomial optimization,” *New Journal of Physics*, vol. 21, no. 7, Article ID 073023, 2019.
- [23] J. J. Sakurai and E. D. Commins, “Modern quantum mechanics, revised edition,” *American Journal of Physics*, vol. 63, no. 93, 1995.
- [24] J. C. Slater, “Atomic shielding constants,” *Physical Review*, vol. 36, no. 1, pp. 57–64, 1930.
- [25] J. C. Slater, “A generalized self-consistent field method,” *Physical Review*, vol. 91, no. 3, pp. 528–530, 1953.
- [26] S. F. Boys, “Electronic wave functions-i. a general method of calculation for the stationary states of any molecular system,” *Proceedings of the Royal Society of London, Series A: Mathematical and Physical Sciences*, vol. 200, no. 1063, pp. 542–554, 1950.
- [27] S. F. Boys, “Electronic wave functions ii. a calculation for the ground state of the beryllium atom,” *Proceedings of the Royal Society of London, Series A: Mathematical and Physical Sciences*, vol. 201, no. 1064, pp. 125–137, 1950.
- [28] R. F. Stewart, “Small Gaussian expansions of slater-type orbitals,” *The Journal of Chemical Physics*, vol. 52, no. 1, pp. 431–438, 1970.
- [29] J. Frank, *Introduction to Computational Chemistry*, John Wiley & Sons, New York, NY, USA, 2017.
- [30] J. C. Slater, “A simplification of the Hartree-Fock method,” *Physical Review*, vol. 81, no. 3, pp. 385–390, 1951.
- [31] P. Lykos and G. W. Pratt, “Discussion on the Hartree-Fock approximation,” *Reviews of Modern Physics*, vol. 35, no. 3, pp. 496–501, 1963.
- [32] J. Casanova, A. Mezzacapo, L. Lamata, and E. Solano, “Quantum simulation of interacting fermion lattice models in trapped ions,” *Physical Review Letters*, vol. 108, no. 19, Article ID 190502, 2012.
- [33] R. Barends, L. Lamata, J. Kelly et al., “Digital quantum simulation of fermionic models with a superconducting circuit,” *Nature Communications*, vol. 6, no. 1, pp. 7654–7657, 2015.
- [34] M. A. Nielsen, *The Fermionic Canonical Commutation Relations and the jordan-wigner Transform*, Vol. 59, School of

Physical Sciences, The University of Queensland, , Queensland, Australia, 2005.

- [35] M. Steudtner and S. Wehner, “Fermion-to-qubit mappings with varying resource requirements for quantum simulation,” *New Journal of Physics*, vol. 20, no. 6, Article ID 063010, 2018.
- [36] C. D. Batista and G. Ortiz, “Generalized Jordan-wigner transformations,” *Physical Review Letters*, vol. 86, no. 6, pp. 1082–1085, 2001.
- [37] J. T. Seeley, M. J. Richard, and P. J. Love, “The bravyi-kitaev transformation for quantum computation of electronic structure,” *The Journal of Chemical Physics*, vol. 137, no. 22, Article ID 224109, 2012.
- [38] A. Tranter, S. Sofia, J. Seeley et al., “The b ravyi- k itaev transformation: properties and applications,” *International Journal of Quantum Chemistry*, vol. 115, no. 19, pp. 1431–1441, 2015.
- [39] A. Tranter, P. J. Love, F. Mintert, and P. V. Coveney, “A comparison of the bravyi-kitaev and Jordan-wigner transformations for the quantum simulation of quantum chemistry,” *Journal of Chemical Theory and Computation*, vol. 14, no. 11, pp. 5617–5630, 2018.
- [40] S. B. Bravyi and A. Y. Kitaev, “Fermionic quantum computation,” *Annals of Physics*, vol. 298, no. 1, pp. 210–226, 2002.